12th International Conference on Fracture Mechanics of Concrete and Concrete Structures
FraMCoS-12
B.L.A. Pichler, Ch. Hellmich, P. Preinstorfer (Eds)

https://doi.org/10.21012/FC12.1266
TT-C2:3

ADVANCEMENTS IN MODELING COMPRESSIVE FRACTURE IN CONCRETE USING CONDENSED HIGH ASPECT RATIO INTERFACE ELEMENTS

MARCELA GIMENES[*], ANDREI F. VILLA DOS SANTOS[*], EDUARDO A. RODRIGUES[*], TÚLIO N. BITTENCOURT[†], LUIS A. G. BITENCOURT JR.[†] AND OSVALDO L. MANZOLI[*]

[*] State University of São Paulo (UNESP)
Department of Civil Engineering, Bauru-Brazil
Av. Eng. Luís Edmundo Carrijo Coube, 14-01, Bauru, Brazil
e-mail: marcela.gimenes@unesp.br; andrei.villa@unesp.br; eduardo.alexandre@unesp.br; osvaldo.l.manzoli@unesp.br

† University of São Paulo (USP)
Department of Structural and Geotechnical Engineering, São Paulo-Brazil
e-mail: tbitten@usp.br; luis.bitencourt@usp.br

Key words: Condensed high aspect ratio elements, Mesh fragmentation technique, Concrete crushing, Shear-compression failure.

Abstract: Accurately predicting concrete failure under compression remains a challenging task in numerical modeling. Manzoli et al. [1] introduced the Mesh Fragmentation Technique, which employs high aspect ratio interface elements between standard mesh elements to define potential crack paths. Building on this, Gimenes et al. [2] proposed an extended approach using a two-layer condensed interface element. This enhancement enables the effective modeling of compressive failure as a combination of debonding (mode-I) and sliding (mode-II) cracking, governed by tensile and shear-frictional constitutive damage models, respectively.
This study highlights recent advancements in using condensed high aspect ratio interface elements to model compressive fracture in concrete. The approach is particularly well-suited for mesoscale modeling, successfully simulating uniaxial compression tests on both conventional and recycled aggregate concrete [2]. It also provides insight into the role of individual phases - aggregate, mortar matrix, and the interfacial transition zone - in the material's response. Additionally, the method can easily simulate varying friction conditions between concrete specimens and steel loading plates.
The technique is evaluated for its suitability in analyzing structural elements, such as reinforced concrete beams, on a macroscale level. The results demonstrate that the model accurately represents failure modes, including concrete crushing and shear-compression. Using two independent damage variables also allows for a clear assessment of the predominant failure mechanisms in different beam configurations.

1 INTRODUCTION

Proper modeling of reinforced concrete (RC) structural members requires understanding the mechanical behavior of concrete and rebars and their interaction [3]. Nowadays, modeling concrete structures remains challenging due to varying failure modes under different loadings

and the size effect. Experimental bending tests indicate that failure modes depend on factors like reinforcement ratio, structural scale, and effective depth ([4], [5], [6]). Shear failure, a sudden and undesirable occurrence, underscores the need for transverse reinforcement [7]. In over-reinforced, deep, and short beams, shear-compression failure may arise due to arch action, especially with a shear span-to-depth ratio below 3.0 [8]. This failure mode is characterized by diagonal cracks and concrete crushing. As the shear span-to-depth ratio increases, failure tends to occur in the compressed region before reinforcement yields, prompting design codes to limit the use of such beams to prevent brittle failures [9].

Due to high experimental testing costs for RC beams, there is ongoing interest in numerical methods to accurately describe failure modes, particularly concrete crushing (CC) and shear-compression (SC) [9]. Numerous numerical methods are used to simulate concrete fractures effectively, depicting the lattice discrete particle model (LDPM), which employs irregular meshing techniques - like random lattice meshes or polygonal/polyhedral assemblage cells - to capture the nonlinear behavior of concrete under various loading conditions ([10], [11]). Additionally, within the finite element method (FEM) framework, approaches such as the extended finite element method (XFEM), phase-field method, and zero-thickness interface element are noteworthy for managing local discontinuities ([12], [13], [14]) The Mesh Fragmentation Technique (MFT), proposed by Manzoli et al. [1], effectively models cracks in quasi-brittle materials, including plain, recycled, and high-strength concrete ([15], [16], [17]). This technique utilizes high-aspect-ratio interface elements to allow for the modeling of multiple crack formations without complex algorithms.

This study presents the application of recent advancements in using condensed high aspect ratio interface elements to model compressive fracture in concrete [2]. This approach employs 2D condensed high aspect ratio elements (HAR-IEs), which integrate two layers of triangular HAR-IEs and incorporate constitutive damage models for tensile and shear-frictional behavior, recently proposed by Gimenes et al. [2]. This methodology accurately represents fractures in mode-I (opening), mode-II (slipping), and the compressive failure of concrete, described as a combined failure mechanism [2]. The condensed HAR-IEs allow for the natural simulation of multiple fracture formations without tracking algorithms, reduce global matrix sizes to lower computational costs, and ensure independent energy dissipation through simple damage models that require only easily obtainable material parameters. In addition, the rebars are represented by truss elements, and their behavior is described using an elastoplastic constitutive model. Coupling finite elements (CFEs) [18][19] describes the interaction between rebars and concrete, employing an appropriate constitutive model. The numerical model is applied to investigate the beam failure modes, especially concrete crushing and shear-compression.

2 MODELING OF REINFORCED CONCRETE

The numerical analysis is carried out within the finite element method framework. The specific models and techniques applied to concrete and reinforcement are described in this section.

2.1 Concrete

A Mesh Fragmentation Technique (MFT) is employed to model crack formation and propagation on concrete, given its quasi-brittle nature. The technique consists of placing high aspect ratio interface elements (HAR-IEs) between standard mesh elements. These elements incorporate continuum constitutive models grounded in damage mechanics, enabling the representation of discontinuity behavior. The kinematics of HAR-IEs align with the continuum strong discontinuity approach, as outlined in prior studies [1]. One of the key advantages of MFT is its capacity to

explicitly simulate the formation and propagation of multiple fractures, including arbitrarily curved ones, without the need for a tracking algorithm. [2].

In this study, a modified version of the MFT is used to model the complex behavior of concrete under compression, following the methodology proposed by Gimenes et al. [2]. Unlike earlier approaches that relied on a single layer of HAR-IEs ([15],[16],[17]), this method introduces a condensed two-layer HAR-IE. For a 2D analysis, this element is described as a four-noded quadrilateral which is internally divided into two layers, each governed by separate tensile and frictional damage constitutive models. Figure 1 illustrates the stages of the MFT, as well as the condensed HAR-IE, named for the static condensation procedure applied to its internal nodes so that only the boundary nodes participate in the assembly of the global matrices [20].

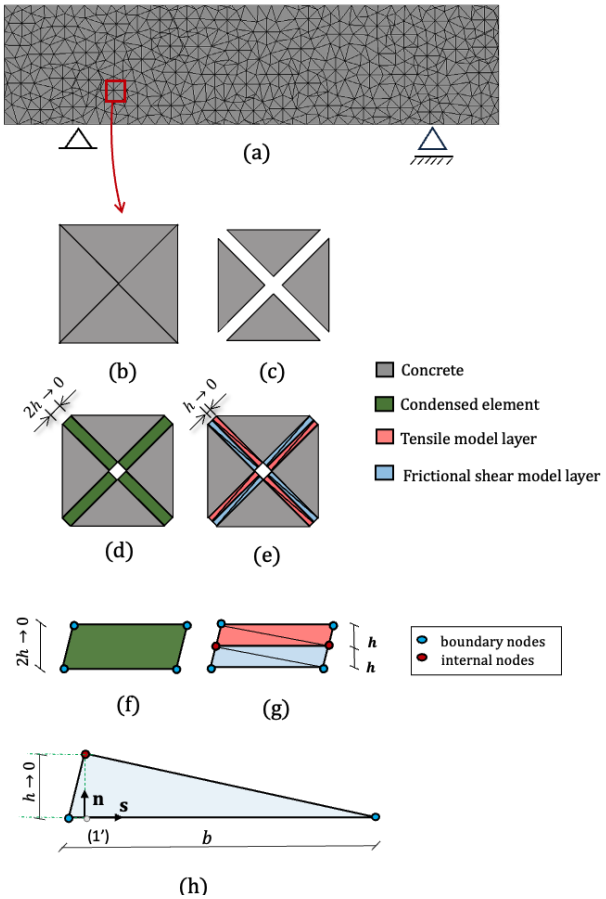

Figure 1: MFT using condensed two-layer HAR-IE: (a) FE mesh; (b) bulk elements; (c) reduction on the size of bulk elements; (d) accommodation of condensed HAR-IEs; (e) internal division of the HAR-IEs into two layers; (f) four-noded condensed HAR-IE; (g) two-layer HAR-IE and (h) HAR triangular element and its local coordinate system (adapted from [2]).

The combination of two damage models at the interfaces enables the simulation of complex behavior such as compressive failure. Moreover, employing independent damage models in each layer ensures accurate energy dissipation corresponding to each failure mode [2].

2.1.1 Tensile damage model

To describe mode-I crack initiation, the tensile damage model associates the effective stress $\bar{\boldsymbol{\sigma}}$ to the nominal stress $\boldsymbol{\sigma}$ by means of a scalar damage variable $d_n \in [0,1]$ as:

$$\boldsymbol{\sigma} = (1 - d_n)\bar{\boldsymbol{\sigma}} \tag{1}$$

$$\bar{\boldsymbol{\sigma}} = \mathbb{C}: \boldsymbol{\varepsilon} \tag{2}$$

where $\mathbb{C}$ is the fourth-order elastic tensor and $\boldsymbol{\varepsilon}$ is the strain tensor. The damage criterion is written in terms of the stress component $\bar{\sigma}_{nn}$, which is defined in the direction of the vector **n** (illustrated in Figure 1-h) as:

$$\bar{\phi}_n = \bar{\sigma}_{nn} - r_n \leq 0 \tag{3}$$

where r_n is the strain-like internal variable, which assumes the maximum value of the corresponding equivalent stress ($\bar{\sigma}_{nn}$) reached during the loading process, from the initial value f_t, which is the tensile strength of the material, so that:

$$r_n = max[\bar{\sigma}_{nn}(k), f_t] \tag{4}$$

with $k \in [0, t]$, being t the pseudo-time in the loading process.

An exponential damage evolution law with adequate softening is considered to represent

the behavior of concrete in tension, so that the stress-like internal variable (q_n) is given by:

$$q_n(r_n) = f_t e^{Ah\left(1-\frac{r_n}{f_t}\right)} \quad (5)$$

The parameters required are the tensile strength of the material, f_t, the thickness of the interface element, h, and the mode-I fracture energy of the material, G_f, which is considered indirectly through the softening parameter $A = \frac{{f_t}^2}{EG_f}$, where E is the Young's modulus of the material. Figure 2 illustrates the evolution law characteristic curve.

The damage variable is calculated as:

$$d_n(r_n) = 1 - \frac{q_n(r_n)}{r_n} \quad (6)$$

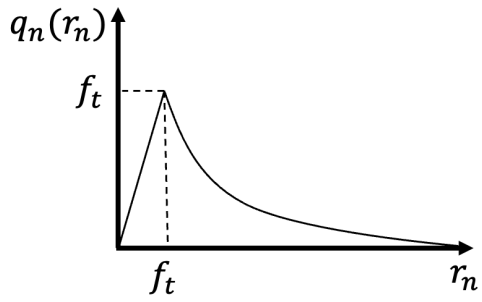

Figure 2: Tensile damage evolution law.

2.1.2 Shear-frictional damage model

To describe mode-II crack initiation, a Coulomb-type isotropic damage model with a scalar damage variable $d_s \in [0,1]$ is employed. Using a local coordinate system (n,s) (illustrated in Figure 1-h), the constitutive equation is written as:

$$\begin{bmatrix}\bar{\sigma}_{nn} & \bar{\sigma}_{ns}\\ \bar{\sigma}_{sn} & \bar{\sigma}_{ss}\end{bmatrix} = \mathbb{C}:\begin{bmatrix}\varepsilon_{nn} & \varepsilon_{ns}\\ \varepsilon_{sn} & \varepsilon_{ss}\end{bmatrix} \quad (7)$$

$$\begin{bmatrix}\sigma_{nn} & \sigma_{ns}\\ \sigma_{sn} & \sigma_{ss}\end{bmatrix} = \begin{bmatrix}\bar{\sigma}_{nn} & 0\\ 0 & \bar{\sigma}_{ss}\end{bmatrix} + (1-\mathrm{d}_s)\begin{bmatrix}0 & \bar{\sigma}_{ns}\\ \bar{\sigma}_{sn} & 0\end{bmatrix} \quad (8)$$

The damage criterion is:

$$\phi_\tau = \|\tau\| + \alpha\sigma_{nn} - q_\tau(r_\tau) \leq 0 \quad (9)$$

where q_τ is a stress-type internal variable, r_τ is strain-type internal variable, and α is the parameter that controls the influence of the normal stress tensor component $\sigma_{nn} \leq 0$.

The criterion in terms of effective stress is:

$$\bar{\phi}_\tau = \|\bar{\tau}\| + \alpha\bar{\sigma}_{nn} - r_\tau \leq 0 \quad (10)$$

The variable r_τ adopts the maximum value of the corresponding equivalent stress ($\|\bar{\tau}\| + \alpha\bar{\sigma}_{nn}$) reached during the loading process, starting from the initial value β, which is considered as the interfacial cohesion of the material:

$$r_\tau = max[\|\bar{\tau}\| + \alpha\bar{\sigma}_{nn}(k), \beta] \quad (11)$$

with $k \in [0, t]$, being t the pseudo-time in the loading process.

The damage variable is calculated according to the following evolution law:

$$d_\tau(r_\tau) = \frac{r_\tau - q_\tau}{r_\tau - \alpha\bar{\sigma}_{nn}} \quad (12)$$

Furthermore, it is considered that the stress-type internal variable q_τ follows a linear law:

$$q_\tau(r_\tau) = \beta + \bar{H}h(r_\tau - \beta) \quad (13)$$

where $\bar{H} < 0$ is the intrinsic softening parameter, illustrated in Figure 3, which is regularized according to the HAR-IE thickness, h, and is related to energy dissipation in mode-II.

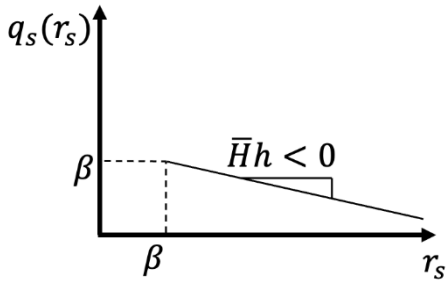

Figure 3: Shear-frictional damage evolution law.

The presented constitutive damage models are integrated using an implicit-explicit integration scheme [21][22].

2.2 Steel reinforcement

The steel reinforcing bars are modeled via truss elements, adopting a one-dimensional perfect elastoplastic constitutive model defined by Young's modulus (E_s) and the yield stress (σ_y).

2.2.1 Coupling finite element and bond-slip law

This work employs triangular four-noded CFEs ([18][19]) to establish an interaction between the finite elements representing concrete and the reinforcement elements, which are defined initially on independent meshes. The coupling strategy for a 2D mesh comprising triangular concrete elements and linear reinforcement elements is illustrated in Figure 4. In this framework, each reinforcement node is treated as a coupled node, denoted as C_{node}. As shown in Fig. 4, node j is integrated into the corresponding CFE located within the adjacent concrete element. The C_{node} exhibits a steel–concrete interaction force arising from the bond (shear) stress τ at the interface area surrounding the reinforcement bar. Additional details on modeling reinforced concrete structures using CFE for discrete representation of reinforcements can be found in Bitencourt et al. [23].

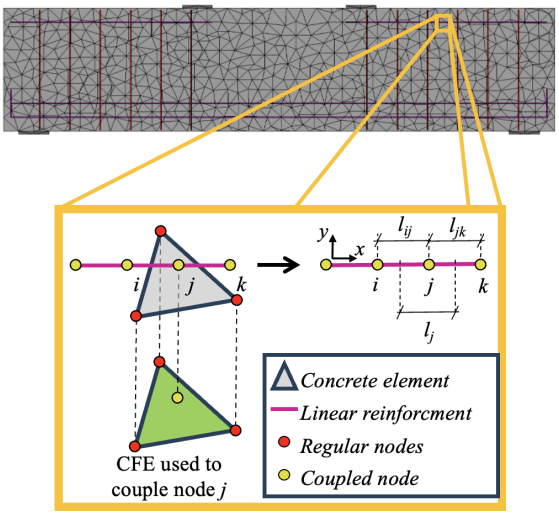

Figure 4: Coupling a linear reinforcement element to its corresponding 2D concrete element via CFE. (Villa dos Santos et al., [20])

3 RESULTS

3.1 Uniaxial compression

Numerical simulation of a uniaxial compression test on a cubic specimen is carried out. The numerical curve is compared to a theoretical curve in order to obtain the parameters that result in 34 MPa of compressive strength in a cubic specimen (which corresponds to approximately 26 MPa in a cylindric specimen). The 100x100x100 mm^3 cube was discretized with 13372 triangular elements measuring 3 mm. The calibrated parameters are employed in the next example involving reinforced concrete beams.

Table 1 summarizes the material concrete parameters, where Young's modulus, Poisson ratio, tensile strength and fracture energy are reported from experimental data [25], while cohesion, friction angle and softening parameters are calibrated.

Table 1: Material parameters for concrete

Young's Modulus (GPa)	30.0
Poisson Ratio	0.2
Tensile strength (MPa)	4.0
Fracture energy (N/m)	133.0
Cohesion (MPa)	9.0
Friction coefficient	0.4
Softening parameter	-0.003

Figure 5 (a) illustrates the theoretical and numerical [24] stress-strain curves, while Figure 5 (b) shows the deformed compression specimen.

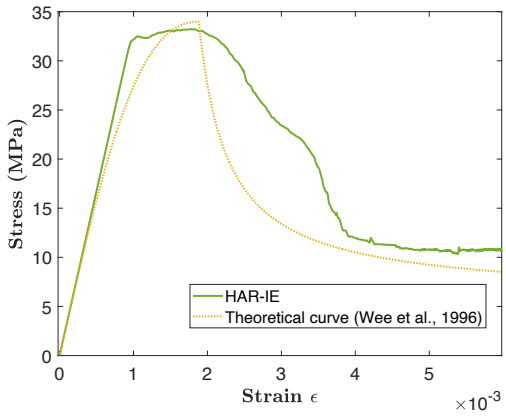

(a)

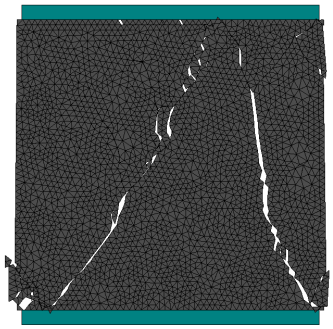

(b)

Figure 5: (a) Stress-strain curve for the uniaxial compressive test and (b) deformed specimen (1.5x amplification factor).

4.2 Reinforced concrete beams

Bresler and Scordelis [25] tested a series of beams with various reinforcement configurations and span conditions, addressing key influencing factors and failure mechanisms. This test series soon became widely recognized as a reference point and has been extensively used to calibrate and validate finite element models of reinforced concrete. More recently, Vecchio and Shim [26] tested the so-called Toronto beams, a replication of the Bresler-Scordelis beams. The purpose was to verify the repeatability of the results and the responses obtained were very similar, supporting their use as benchmark data. In the present study, two of those beams are simulated in order to demonstrate the model capability of predicting different failure modes. The respective beams are illustrated in Figure 6.

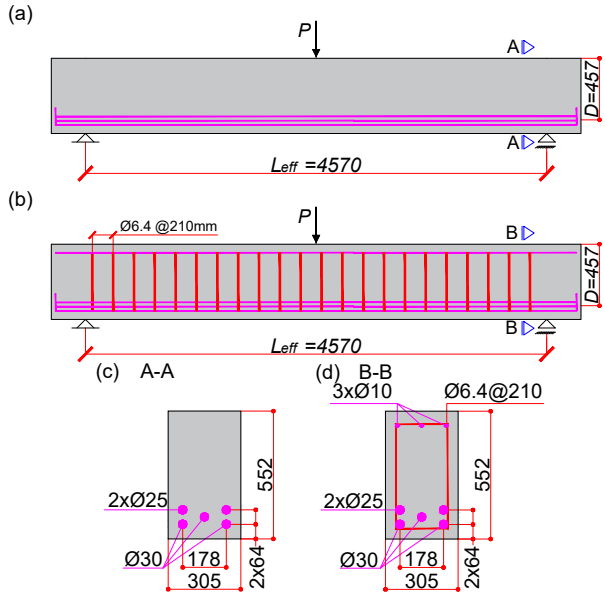

Figure 6: Geometry and reinforcement arrangements for beams (a) OA2 and (b) A2.

The input parameters for arrangements and material properties are referenced in the work of [26]. Both beams have the same cross-section; however, beam "OA2" does not have web reinforcement, while beam "A2" has it. Concrete compressive strength is 26 MPa and Young's modulus is 30 GPa. Thus, the same parameters from Table 1 are used in the numerical simulation. The beams were modeled in 2D using triangular finite elements with a size of 12.5 mm. The resulting number of nodes and elements after mesh fragmentation and coupling procedure for beam OA2 was 137209 and 118567, respectively. For beam A2, the number of nodes was 138779, and the number of elements was 120189.

Figure 7 and Figure 8 illustrate the failure modes for each case. Beam OA2 (without web reinforcement) exhibited a shear failure, while the beam A2 (with web reinforcement) experienced concrete crushing. Besides, both numerical responses are very similar to the experimental failure modes obtained by [26].

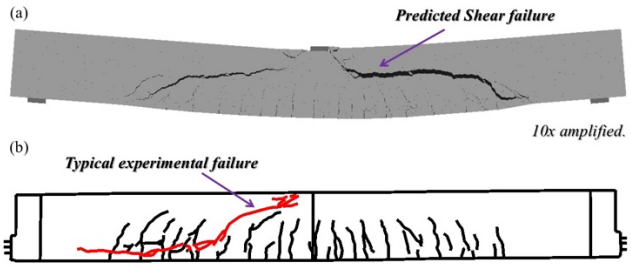

Figure 7: Failure mode of beam OA2 (a) numerically predicted and (b) experimentally observed (adapted from [26]).

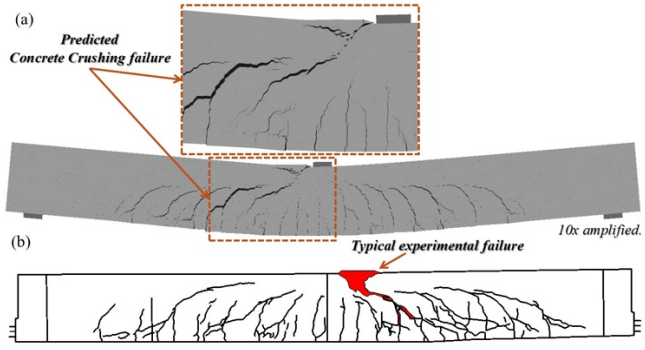

Figure 8: Failure mode of beam A2 (a) numerically predicted and (b) experimentally observed (adapted from [26]).

Figures 9 and 10 depict the load *versus* vertical displacement curves, comparing the results of the proposed numerical approach with the experimental data from Bresler-Scordelis [25] and Toronto [26] beams. Additionally, a numerical curve from Vecchio and Shim is included for comparison.

For beam OA2, the proposed approach produced results that closely matched the reference data. For beam A2, while the peak load obtained was nearly identical to the reference cases, the failure was more brittle compared to the experimental results.

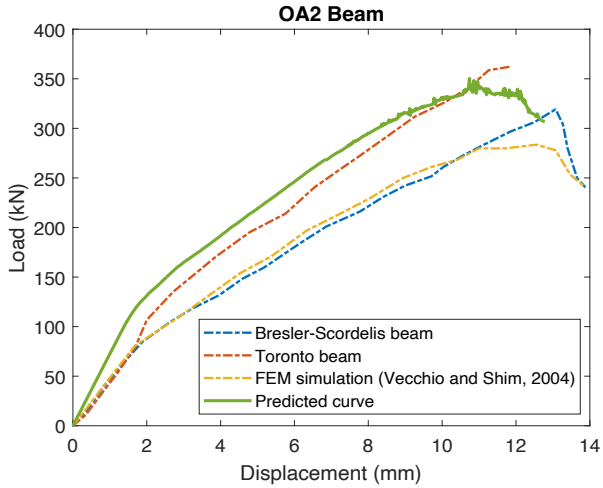

Figure 9: Load *versus* displacement curves of beam OA2: (a) numerically predicted and (b) experimentally observed (adapted from [26]).

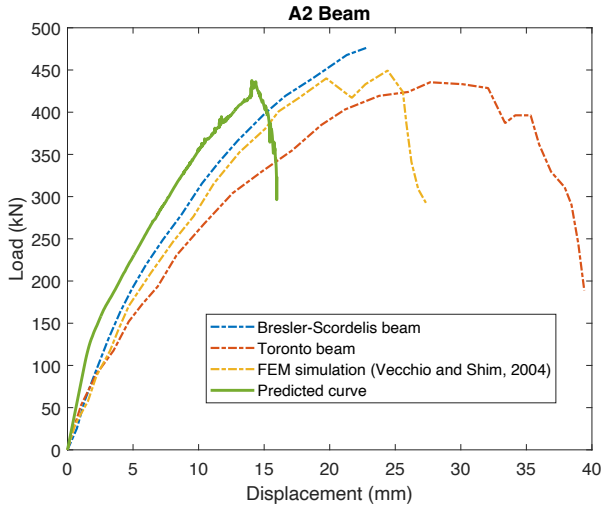

Figure 10: Load *versus* displacement curves of beam A2: (a) numerically predicted and (b) experimentally observed (adapted from [26]).

5 CONCLUSIONS

This work presents a new methodology to simulate complex fracture propagation on reinforced concrete elements using the combination of simple constitutive models based on damage mechanics theory.

A two-layer HAR-IE ruled by tensile and shear-frictional damage models is employed requiring only a few material parameters.

The parameters obtained from the calibration of a uniaxial compression test were suitable for the analysis of real-scale reinforced concrete elements.

Different failure modes were obtained for beams with different reinforcement arrangements. The numerical response was aligned to the experimental, where beams without web reinforcement exhibited a shear failure, while the beams with web reinforcement experienced concrete crushing.

REFERENCES

[1] Manzoli, O.L., Maedo, M.A., Bitencourt Jr., L.A.G. and Rodrigues, E.A., 2016. On the use of finite elements with a high aspect ratio for modeling cracks in quasi-brittle materials. Engineering Fracture Mechanics, 151-170.

[2] Gimenes, M., Rodrigues, E.A., Bitencourt Jr, L.A.G. and Manzoli, O.L., 2023. 2D mesoscale modeling of compressive fracture in concrete using a mesh fragmentation technique. International Journal of Solids and Structures, 260, 112031.

[3] Cervenka J., Jendele L. Finite element modelling of reinforcement with bond. Comput Methods Appl Mech Engrg, 84 (2006), pp. 1780-1791.

[4] Carpinteri A., Ventura G., Carmona J., et al. Flexural to shear and crushing failure transitions in RC beams by the bridged crack model. Fract Mech Concr Struct, 2 (2007), pp. 677-684. Proc. of FraMCoS-6.

[5] Syroka-Korol E., Tejchman J. Experimental investigations of size effect in reinforced concrete beams failing by shear. Eng Struct, 58 (2014), pp. 63-78.

[6] Corrado M., Ventura G., Carpinteri A. Experimental evidences of flexural to shear to crushing failure mode transition in reinforced concrete beams without stirrups. Eng Struct, 271 (2022), Article 114848.

[7] Bazant Z.P., Kazemi M.T., et al. Size effect on diagonal shear failure of beams without stirrups ACI Struct J, 88 (3) (1991), pp. 268-276.

[8] Mak M.W.T., Lees J.M. Arch action in reinforced concrete subjected to shear. Eng Struct, 274 (2023), Article 115096.

[9] Marzec I., Tejchman J. Experimental and numerical investigations on RC beams with stirrups scaled along height or length. Eng Struct, 252 (2022), Article 113621.

[10] Jin C., Buratti N., Stacchini M., Savoia M., Cusatis G. Lattice discrete particle modeling of fiber reinforced concrete: Experiments and simulations. Eur J Mech A Solids, 57 (2016), pp. 85-107.

[11] Bolander J.E., Eliáš J., Cusatis G., Nagai K. Discrete mechanical models of concrete fracture Eng Fract Mech, 257 (2021), Article 108030.

[12] Du X., Jin L., Ma G. Numerical modeling tensile failure behavior of concrete at mesoscale using extended finite element method. Int J Damage Mech, 23 (7) (2014), pp. 872-898.

[13] Yang L., Yang Y., Zheng H. A phase field numerical manifold method for crack propagation in quasi-brittle materials. Eng Fract Mech, 241 (2021), Article 107427.

[14] Segura J., Carol I. Numerical modelling of pressurized fracture evolution in concrete using zero-thickness interface elements. Eng Fract Mech, 77 (9) (2010), pp. 1386-1399.

[15] Rodrigues E.A., Manzoli O.L., Bitencourt Jr. L.A., Bittencourt T.N. 2D mesoscale model for concrete based on the use of interface element with a high aspect ratio. Int J Solids Struct, 94–95 (2016), pp. 112-124.

[16] Gimenes M., Rodrigues E.A., Maedo M.A., Bitencourt L.A.G., Manzoli O.L. 2D crack propagation in high-strength concrete using multiscale modeling. Multisc Sci Eng, 2 (2) (2020), pp. 169-188.

[17] Rodrigues E.A., Gimenes M., Bitencourt Jr. L.A., Manzoli O.L. A concurrent multiscale approach for modeling recycled aggregate

concrete. Constr Build Mater, 267 (2021), Article 121040.
[18] Bitencourt Jr, L. A., Manzoli, O. L., Prazeres, P. G., Rodrigues, E. A., & Bittencourt, T. N., 2015. A coupling technique for non-matching finite element meshes. Computer methods in applied mechanics and engineering, 290, 19-44.
[19] Bitencourt Júnior, Luís Antônio Guimarães. Numerical modeling of failure processes in steel fiber reinforced cementitious materials. Doctoral Thesis. Polytechnic School at the University of Sao Paulo. doi:10.11606/T.3.2014.tde-16112015-50922.
[20] Villa dos Santos, A. F., Gimenes, M., Rodrigues, E. A., Cleto, P. R., and Manzoli, O. L., 2025. Modeling different modes of failure in reinforced concrete beams combining tensile and shear-frictional damage models and bond–slip coupling for non-matching reinforcement and fragmented concrete meshes. Engineering Structures, 323, 119265.
[21] Oliver, J., Huespe, A. E., & Cante, J. C., 2008. An implicit/explicit integration scheme to increase computability of non-linear material and contact/friction problems. Computer Methods in Applied Mechanics and Engineering, 197(21-24), 1865-1889.
[22] Prazeres, P.G.C.; Bitencourt, L.A.G.; Bittencourt, T.N.; Manzoli, O.L. A modified implicit-explicit integration scheme: an application to elastoplasticity problems. Journal of the Brazilian Society of Mechanical Sciences and Engineering, v.38, p.151-161, 2016.
[23] Bitencourt, L.A.G.; Manzoli, O.L.; Trindade, Y.T.; Rodrigues, E.A.; Dias-da-Costa, D. Modeling reinforced concrete structures using coupling finite elements for discrete representation of reinforcements. Finite Elements in Analysis and Design, v. 149, p. 32-44, 2018.
[24] Wee, T.H., Chin, M.S., Mansur M.A. 1996. Stress-strain relationship of high-strength concrete in compression. J Mater Civ Eng 8(2):70–6.
[25] Bresler, B., and Scordelis, A.C., 1963. Shear strength of reinforced concrete beams. ACI Journal Proceedings (Vol. 60, No. 1, pp. 51-74).
[26] Vecchio, F. J., and Shim, W., 2004. Experime
ntal and analytical reexamination of classic concrete beam tests. Journal of Structural Engineering, 130(3), 460-469.